DHI WATER & ENVIRONMENT

MIKE 21C RIVER MORPHOLOGY

A Short Description

INTRODUCTION TO THE SYSTEM

MIKE 21C is a generalised mathematical modelling system for the simulation of the hydrodynamics of vertically homogenous flows, and for the simulation of sediment transport. The modelling system has the capability of utilising both a rectilinear and a curvilinear computational grid.

The modelling system, which is a part of the MIKE 21 software package from DHI Water & Environment, is composed of a number of modules relevant to sediment and morphology studies in rivers:

- Hydrodynamic module
- Advection-dispersion module
- Sediment transport module
- Flow resistance module
- Bank erosion module
- Large scale morphological module

These features are described in general terms in the following sections.

The model components can run simultaneously, thus incorporating dynamic feedback from changing hydraulic resistance, bed topography and bank lines to the hydrodynamic behaviour of the river.

For pre- and post-processing of input and output, the MIKE 21 PP-module (pre- and post-processor) from the MIKE 21 family is used. Special utility programmes have been developed to handle data in a curvilinear grid format:

- Graphics-based and menu-driven grid generator to create curvilinear grids and model bathymetries
- Result-Viewer for 2D contour and vector plots as well as time series plot
- Utility tools to extract time series, profiles, width-integrated discharge etc.

Application areas

The MIKE 21C is used for simulation of two-dimensional free surface flow and sediment transport in rivers where stratification can be neglected and where an accurate description of the flow along the banks as well as helical three-dimensional flow is important. Typical model applications comprise

- Protection schemes against bank erosion and bed scour measures to reduce or manage shoaling
- Structures including e.g. weirs, groynes, barrages, bendway weirs
- Alignments and dimensions of navigation channels for minimizing capital and maintenance dredging
- Sedimentation of water intakes, outlets, locks, harbors, reservoirs
- Bridge, tunnel and pipe line crossings
- Restoration plans for optimal environmental habitats in channel-floodplain systems
- Monitoring networks based on morphological forecasting

ELLIPTIC GRID GENERATOR

The general version of the MIKE 21 is based on a rectilinear computational grid. For modelling of the open sea, and most estuaries and coastal applications, such a grid provides sufficient accuracy. In river application, however, an accurate resolution of the boundaries is required which necessitates for the use of curvilinear or unstructured grids. Curvilinear grids have the advantage over the unstructured grids that the computational schemes are much faster.

The benefits of using a curvilinear computational grid compared to a rectilinear grid are visualised in Figure 1, where a river reach is described in both a curvilinear and a rectilinear grid. In this example, the discretization in the curvilinear grid is based on 210 computational points, whereas the rectilinear model uses 228 active (water) points. The curvilinear model provides a much better resolution of the flow near the boundaries and thereby a higher modelling accuracy. Bigger time step can be used in the curvilinear model because grid lines follow the streamlines. In the rectilinear model, a total of 900 points is defined and stored, whereas for the curvilinear model, only 270 points are defined. Thus, the required storage capacity is relatively larger in a rectilinear model.

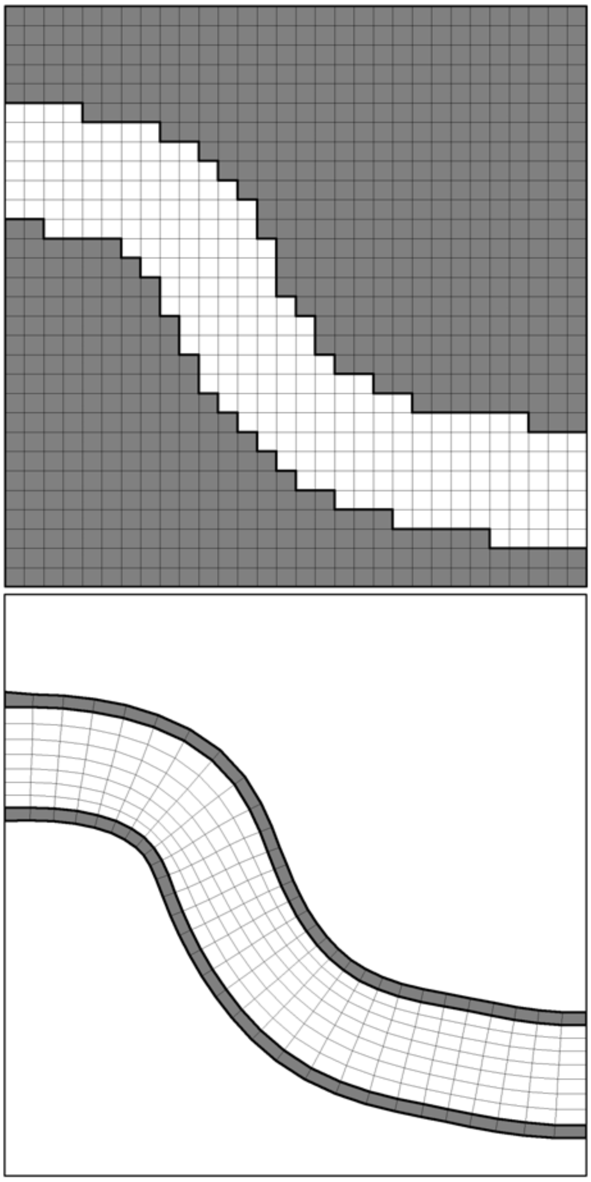

Figure 1 Schematisation of a river in rectilinear and curvilinear grid.

MIKE 21C is based on a so-called orthogonal curvilinear grid. This is created with a graphical based grid generator, which solves a set of elliptic partial differential equations. The advantage of using an orthogonal grid is that the finite difference equations describing the two-dimensional flow become substantially simpler than if a general (non-orthogonal) curvilinear grid was applied. This implies that the numerical scheme becomes more accurate with an orthogonal grid and that the computational speed of the engine improves.

The orthogonal curvilinear grid used in MIKE 21C is obtained from the following elliptic partial differential equations:

$$\frac{\partial}{\partial s}\left[g\frac{\partial x}{\partial s}\right]+\frac{\partial}{\partial n}\left[\frac{1}{g}\frac{\partial x}{\partial n}\right]=0$$

$$\frac{\partial}{\partial s}\left[g\frac{\partial y}{\partial s}\right]+\frac{\partial}{\partial n}\left[\frac{1}{g}\frac{\partial y}{\partial n}\right]=0$$

where

x,y Cartesian co-ordinates

s,n curvilinear co-ordinates (anti-clockwise system)

g "weight" function

The weight function is a measure of the ratio between the grid cell length in the s- and the n-direction, respectively.

The boundary condition for this system is the non-linear orthogonality condition:

$$\frac{\partial x_b}{\partial s}\frac{\partial x_b}{\partial n}+\frac{\partial y_b}{\partial s}\frac{\partial y_b}{\partial n}=0$$

$$f(x_b, y_b)=0$$

where the former expresses the condition of orthogonality and the latter expresses the location of grid points (x,y) on a specific curve describing the boundary. A strongly implicit method is employed for solving the partial differential equations with a special Newton-Raphson procedure for the boundary conditions, see Stone (1968).

Generation of an orthogonal curvilinear grid is an iterative process in which boundaries are smoothened and weight functions are adjusted until the computational grid is judged to be sound, i.e. without too large gradients in grid cell spacing and curvature of grid lines. Figure 2 shows an example of a curvilinear grid obtained with the elliptic grid generator. The graphical based grid generator offers a number of flexible tools to tailor the grid to the model area, for instance around an in-channel bar.

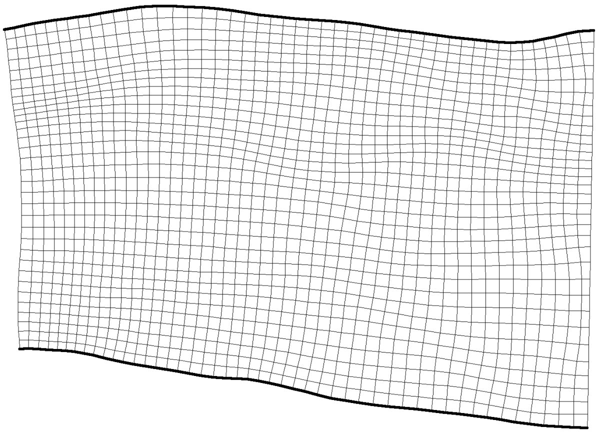

Figure 2 Example of curvilinear grid. The weight function causes the grid to be concentrated in the deeper parts (depth adaptive grid)

Input

Input for the grid generator is

- Boundary lines, either imported from ASCII files containing (x,y) co-ordinates or digitised directly on top of a geo-referenced bitmap within the grid generator
- Specification of the required number of grid points along the river, and across the river
- River bed levels, defined as a set of discrete values with bed level z at given (x,y) co-ordinates. Data can be imported from an ASCII file or from another MIKE 21 dfs-file.

Output

Output from the grid generator is two files, which is required for a curvilinear model setup

- A 2D map of the co-ordinates of every corner point in each grid cell in the curvilinear mesh. (This file is a standard dfs2 file with two items x and y).
- A 2D map of the river bed level at every centre point in the each grid cell in the curvilinear mesh. (This standard dfs2 file is similar to a bathymetry file in a general MIKE 21 setup).

HYDRODYNAMIC MODEL

The hydrodynamic model simulates the water level variation and flows in rivers and estuaries. Model simulations are based on a curvilinear computational grid covering the area of interest. The MIKE 21 hydrodynamic model has been under continuous development at DHI Water & Environment since 1970 whereas the curvilinear version of MIKE 21 using the same solution methods was developed in 1990.

Basic Equations

The hydrodynamic model solves the full dynamic and vertically integrated equations of continuity and conservation of momentum (the Saint Venant equations) in two directions. The following effects can be included in the equations when used for river applications:

- flow acceleration
- convective and cross-momentum
- pressure gradients (water surface slopes)
- bed shear stress
- momentum dispersion (through e.g. the Smagorinsky formulation)
- flow curvature and helical flow

The curvature of the grid lines gives rise to additional terms in the partial differential equations for the flow. The equations solved in MIKE 21C are:

$$\frac{\partial p}{\partial t}+\frac{\partial}{\partial s}\left(\frac{p^2}{h}\right)+\frac{\partial}{\partial n}\left(\frac{pq}{h}\right)+2\frac{pq}{hR_n}+\frac{p^2-q^2}{hR_s}+gh\frac{\partial H}{\partial s}+\frac{g}{C^2}\frac{p\sqrt{p^2+q^2}}{h^2}=RHS$$

$$\frac{\partial q}{\partial t}+\frac{\partial}{\partial s}\left(\frac{pq}{h}\right)+\frac{\partial}{\partial n}\left(\frac{q^2}{h}\right)+2\frac{pq}{hR_s}+\frac{q^2-p^2}{hR_n}+gh\frac{\partial H}{\partial n}+\frac{g}{C^2}\frac{q\sqrt{p^2+q^2}}{h^2}=RHS$$

$$\frac{\partial H}{\partial t}+\frac{\partial p}{\partial s}+\frac{\partial q}{\partial n}-\frac{q}{R_s}+\frac{p}{R_n}=0$$

where

s,n	co-ordinates in the curvilinear co-ordinate system
p,q	mass fluxes in the s- and n-direction, respectively
H	water level
h	water depth
g	gravitational acceleration
C	Chezy roughness coefficient
R_s, R_n	radius of curvature of s- and n-line, respectively.

RHS The right hand side describing a.o. Reynold stresses (see MIKE 21 Hydrodynamic Module)

Solution Technique

The equations are solved by implicit difference techniques with the variables defined on a space staggered computational grid as shown in Figure 3.

Two solution algorithms exist in MIKE 21C. The first is the “classical” ADI (alternate direction iteration) scheme as applied in the general MIKE 21, which is applicable for highly dynamic flow. The other scheme is based on quasi-steady assumptions and is a predictor-corrector algorithm that originates from methods for incompressible fluid flow (Michelsen, 1989). The quasi-steady solver is particular suitable for slowly varying flow conditions in long-term simulations.

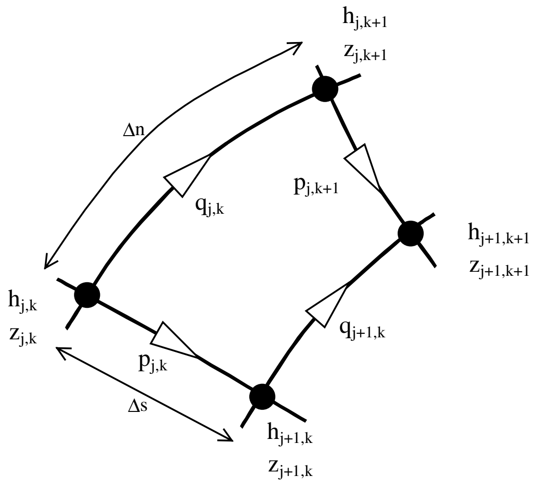

Figure 3 Space staggered grid used in the hydrodynamic model of MIKE 21C

Establishing a model setup

The setting up of a hydrodynamic river model using MIKE 21C involves the following three steps:

- The extent of the modelling area is selected and the computational grid is designed for the river as described in the previous section. The extent of modelling areas can vary from few hundred metres to more than 100 km. The grid size depends on the channel width (typically not less than 10 points across), the depth (not less than say two times the maximum depth), flow direction (grid spacing in the longitudinal direction is often two-three times the spacing across). Grid spacing of 100m x 50m for larger rivers and 30m x 10m for smaller rivers is typical.The bed levels are entered into the computational grid. Various utilities in the grid generator perform conversions, interpolation, extrapolation, smoothening etc.

- The simulation period is planned and the boundary conditions are specified, for instance a time series of discharge at the inflow boundary, and a time series of water level at the downstream model boundary. The typical length of simulation periods varies from days to several months (full dynamic) and several years (quasi-steady).

- Finally, the initial conditions in terms of water levels and fluxes at the beginning of the simulation are defined. This can be done in different ways with for instance a hot-start or a warm-up period.

Calibration

The calibration process for the MIKE 21C hydrodynamic model involves tuning of a number of calibration factors, first of all the bed resistance (Chezy or Manning number) and the Eddy viscosity (constant, 2D map or Smagorinsky formulation). All the calibration factors have a physical meaning and should not be arbitrarily given values outside their realistic ranges to obtain agreement with observed data. In Figures 4 and 5, some computational examples are presented.

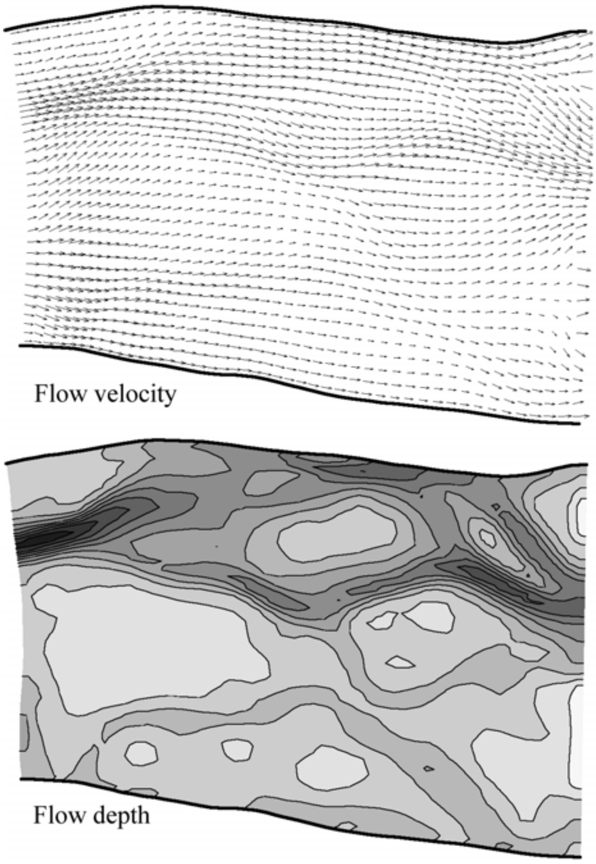

Figure 4 Simulated flow pattern in a braided river (Brahmaputra River). The computational grid is depicted in Figure 2.

Input

The input for the menu-driven setup editor is

- 2D map of the curvilinear mesh and a 2D map of the bed levels (from the grid generator)
- Time series of discharge at the upstream boundary and water level at the downstream boundary (ASCII file format, Excel or similar)
- 2D map of the initial surface water elevation (from the grid editor), or a constant

Output

The output from a MIKE 21C hydrodynamic model comprises the following parameters in a predefined number of time steps during the simulation period

- 2D map of water depth
- 2D map of water flux in two directions (contours or vectors)

Derived results, which can be extracted by a number of graphics based tools are

- 2D maps of flow velocity in two directions (contours or vectors),
- and water surface elevation
- Time series and profiles in selected points/lines of discharge, water level, flow velocity, depth etc.

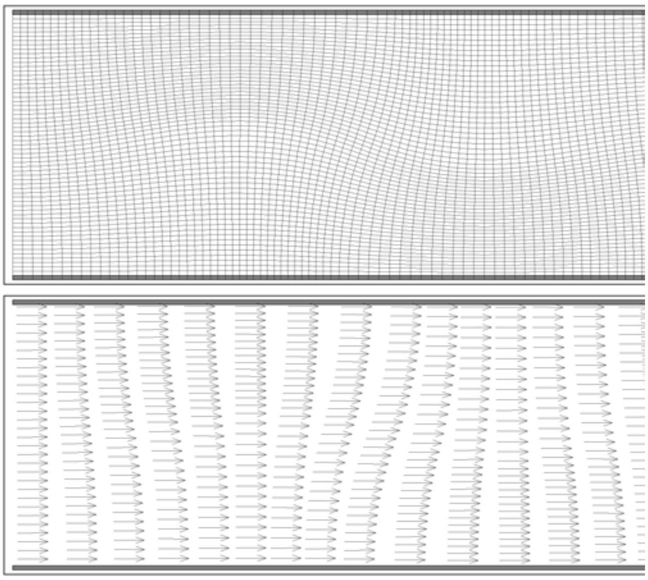

Figure 5 Schematical example of a curvilinear grid and simulated flow distribution in a straight rectangular channel. The example shows effect of curvilinear terms.

SEDIMENT TRANSPORT

Helical Flow

Helical flow is a principal secondary flow phenomenon in rivers. Whilst it does not have any strong influence on the general flow pattern in rivers with large width-depth ratios, it has a significant influence on the sediment transport direction and hence the morphological changes in the river channel (see Olesen, 1987). The helical flow is, therefore, calculated in connection with sediment transport simulations when larger scale morphology is modelled. It is an important ingredient in the development of bend scour, confluence scour, and in formation of point bars as well as alternating bars.

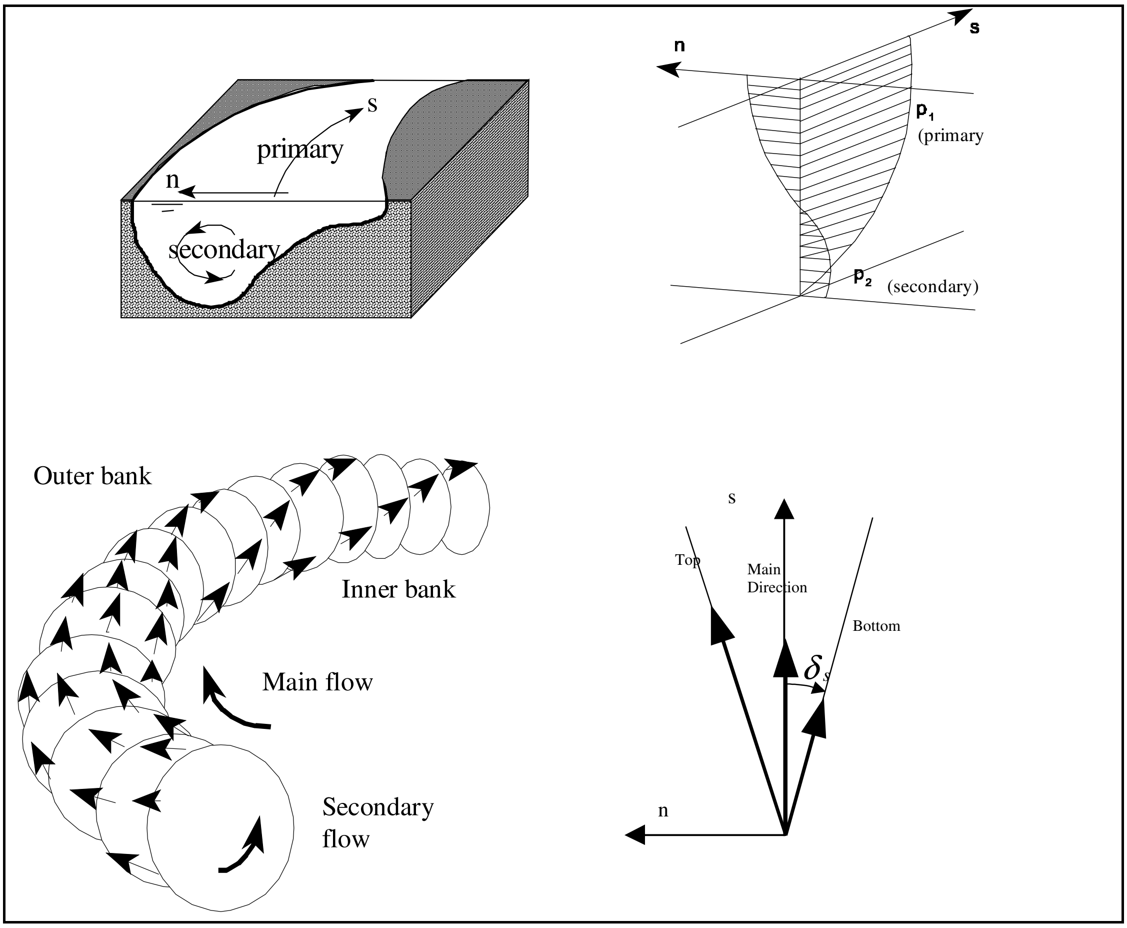

Figure 6 Theoretical illustrations of helical (secondary) flow in a river bend.

The helical flows occur in curved flows, especially in river bends. It arises from the imbalance between the pressure gradient and the centripetal acceleration working on a water particle moving along a curved path. Near the riverbed the helical flow is directed towards the centre of flow curvature. The magnitude of the helical flow (i.e. the transverse flow velocity component) rarely exceeds 5-10 % of the main flow velocity in natural rivers. A typical helical flow pattern is shown in Figure 6.

Assuming a logarithmic main flow velocity distribution over the vertical and a parabolic eddy viscosity distribution, the magnitude of the secondary flow can be shown to be proportional to the main flow velocity, the depth of flow and the curvature of the main flow stream lines. In MIKE 21C, the streamline curvature is calculated explicitly from the depth integrated flow field. The gradual adaptation of secondary (helical) flow to changing curvature is accounted for by solving a first order differential equation along the stream lines with the strength of the helical flow as the dependent variable (see also de Vriend, 1981). The strength of the helical flow is used to determine the direction of both bed and suspended load.

With streamlines of radius R_s of curvature and depth H, the helical flow intensity can be expressed as (U is the main flow speed, C is Chezys number):

$$i_h = \chi_e \cdot U$$

where the helical flow strength was first derived by Rozowsky, 1957:

$$\chi_e = \frac{2}{\kappa^2}\left(1 - \frac{\sqrt{g}}{\kappa \cdot C}\right) \cdot \frac{H}{R_s}$$

Transport formulae

In connection with detailed (two-dimensional) mathematical modelling of sediment transport and morphology in rivers with large suspended load transports, it is necessary to distinguish between bed and suspended load in order to:

- simulate the dynamic development of bed form dimensions
- account for the effect of helical flow as well as the bed slope on the sediment transport direction

The relatively simple total load sediment transport formulas, such as Engelund & Hansen, 1967 and Ackers & White, 1973 can therefore not be used for river applications with consideration of helical flow and bed slope without a separate specification of how the sediment is distributed between bed load and suspended load. It is possible, though, to run simulations by MIKE 21C with a total transport formula only by disregarding the effect of helical flow and bed slope.

The sediment transport models developed by Engelund & Fredsoe, 1976, and van Rijn, 1984, which distinguish between bed and suspended load form the basis for the sediment transport description in MIKE 21C. The specification of the sediment transport formulas is, however, very flexible. Specially developed sediment transport formulas (determined from for instance field measurements) can be specified separately for bed load and suspended load, respectively. With this flexible sediment transport formulation, it is also possible to select formulas like Engelund-Hansen, Smart-Jaeggi, and Meyer-Peter.

If the suspended sediment transport is negligible compared to the bed load transport, the suspended sediment model can be switched off, so only a bed load model (or a total load model) is employed.

Bed Load

In MIKE 21C, the bed load transport is calculated explicitly from one of the selected formulas, eg. Engelund-Fredsøe, van Rijn, or Meyer-Peter. These formulas relate the transport rate to the bed shear stress and the grain diameter.

On a horizontal bed, the transport direction will coincide with the direction of the bed shear stress. The direction of the bed shear stress may, however, deviate from the direction of the depth-averaged flow due to the helical flow as described in a previous section. If δ is the angle of deviation due to the helical flow and χ is the helical flow strength, the following relation exists:

$$\tan\delta = \chi$$

On sloping beds, the gravity will have influence on the transport direction as sketched in Figure 7. The description of the effect of gravity and bed slope on the transport direction is as described below in MIKE 21C. Due to bed slope effects the angle of deviation, α, is (G and a are coefficients, I transverse bed slope):

$$\tan\alpha = G \cdot \theta^{-a} \cdot I$$

The bed slope is I, the angle of deviation is α, θ is non-dimensional bed shear stress and *G* and *a* are calibration parameters. Typical values of G and *a* are 0.66 and 0.5, respectively. Most of these relations have, however, only been verified against data from laboratory tests and are, therefore, not necessarily applicable to natural rivers with large suspended load, see also Talmon/Struiksma/van Mierlo 1995. The applicable relation is therefore often determined via calibration of the model. Corrections in the calculated bed load transport due to sloping river bed in the main flow direction is also done in MIKE 21C.

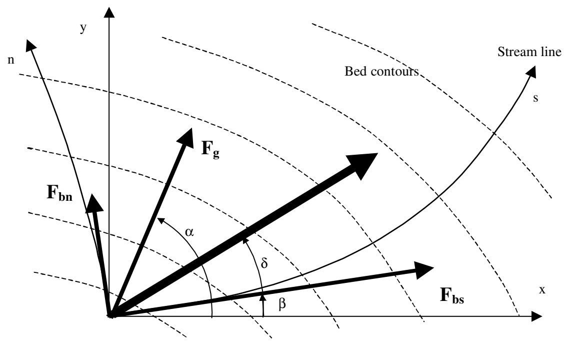

Figure 7 Shear stress on bed load sediment particles is composed of three "drag" components: Force due to main flow F_{bs}*, force due to secondary flow* F_{bn}*, force due to gravity on a sloping riverbed.*

Suspended Load

Standard methods for calculation of suspended load are not applicable in the case of detailed (ie. high resolution) modelling of rivers. It is necessary to include the time-space lag in the sediment transport response to changes in local hydraulic conditions. Consider, for instance, an increase of flow velocity in a river (eg. a constriction). As the flow velocity increases, the entrainment at the river bed will increase correspondingly, but it will take some time (and hence some distance) for the sediment entrained at the bottom to disperse all through the water column. This means that the actual suspended load is not only a function of local hydraulic conditions, as it is normally assumed in most mathematical sediment transport models, but it is also a function of what takes place upstream and earlier in time.

A relevant time scale for the time lag (T) is the settling time for a sediment grain in the water column:

$$T = h_*/w_s$$

where h_* is the effective fall height (depends on the shape of the vertical concentration profile and, thus, on the fall velocity and eddy dispersion) and w_s is the fall velocity.
Correspondingly, a length scale for the space lag is

$$L = T \cdot U$$

where U is the flow velocity. Assuming h_*=8 m, w_s=0.02 m/s, U =2 m/s, the time and length scales are 400 s and 800 m, respectively. Consequently, the space lag is important for river applications .

The space lag effect is modelled in MIKE 21C by a depth-averaged convection-dispersion model which represents the transport and the vertical distribution of suspended solids and flow. This model is an extension of the model first developed for one dimension by Galappatti (1983) and later in two dimensions by Wang (1989). The model by Wang, however, was primarily developed for estuarine applications and did not include the effect of helical flow. This effect is essential in the case of river applications because the suspended load direction will be different from the main flow direction due to helical flow, as shown in Figure 7.

The secondary flow profile is computed in MIKE 21C and used together with the primary flow profile and the concentration profile when the suspended load is integrated over the depth. As the concentration is highest near the river bed, the suspended load transport will be deflected towards the centre of flow curvature. In contrast to bed load, the transverse river bed slope does not influence the direction of suspended load transport.

The depth averaged convection-dispersion model requires an expression for the equilibrium concentration. The models by eg. Engelund & Fredsøe (1982) or van Rijn (1984) can be used for that purpose. The empirical formulas implemented in MIKE 21C can also be used assuming that the equilibrium concentration equals the suspended load transport divided by the water flux.

Supply-limited sediment transport

An important feature of the MIKE 21C is to simulate supply-limited sediment transport, i.e. a sediment layer on the riverbed of finite thickness. Below a pre-defined equilibrium thickness (usually associated with the height of sand dunes in sandy rivers), the sediment transport is reduced according to the availability of sediment. Erosion can only take place, as long as there is sediment available on the riverbed. A 2D map of the initial sediment layer thickness can be defined. The feature is used in connection with for instance representation of river training works (revetments, groynes, weirs etc.) or fine sediment transport over a rock bed.

Graded sediment transport

The MIKE 21C is capable of simulating several fractions of sediment, each with a characteristic grain size. Each grain fraction is simulated separately with due consideration to the inter-action between the various grain components at the riverbed (shielding, armouring). Thus, the graded sediment model is applied in conjunction with defined sediment layers, each composed with defined percentages of each sediment fraction. With this model, it is possible to simulate the sorting in space and time of graded sediment.

Cohesive sediment

A simple version of cohesive sediment description is included in the MIKE 21C sediment transport model allowing the user to specify sediment fractions in a graded sediment model over a wide range from mud to silt, sand, gravel and cobbles. This is relevant for instance in connection with modelling of reservoir sedimentation with larger particles depositing in the upper part of the reservoir and finer particles depositing in the lower (and deeper) part of the reservoir.

Input

To summarise, the main input parameters for the MIKE 21C sediment transport model is

- Grain size (2D map or constant in the enture area)
- The percentage and grain size for all fractions in case a graded sediment model is applied
- Initial concentration of sediment (if required. Default is nil).
- Transport formulae for bed load and/or suspended load

The main calibration coefficients are

- Coefficient for helical flow intensity
- Calibration factors for sediment formulae
- Dispersion coeffients

Output

The output parameters for the MIKE 21C sediment transport model in a predefined number of time steps during the simulation period are

- 2D map of concentration of suspended sediment
- 2D map of bed load transport, suspended load transport and total load transport in two directions (contours or vectors)
- 2D map of net sedimentation

Derived results, which can be extracted by a number of graphics based tools are

- Time series and profiles in selected points/lines of concentration and sediment transport rates.

ALLUVIAL RESISTANCE

It is far more complex to determine the hydraulic resistance in alluvial rivers than in channels with a fixed bed. This is because a large part of the hydraulic resistance in alluvial rivers is caused by bed form drag. The bed forms have a configuration determined by the sediment transport and flow. The hydraulic resistance will therefore exhibit both temporal and spatial variations.

Generally, the hydraulic resistance is divided into that caused by drag on the bed forms (form friction) and due to shear forces on the bed (skin friction). The skin friction is relatively accurately determined from a logaritmic boundary layer equation based on the median grain size of the bed. The form friction, however, can only be determined analytically if the size of the bed forms is known.

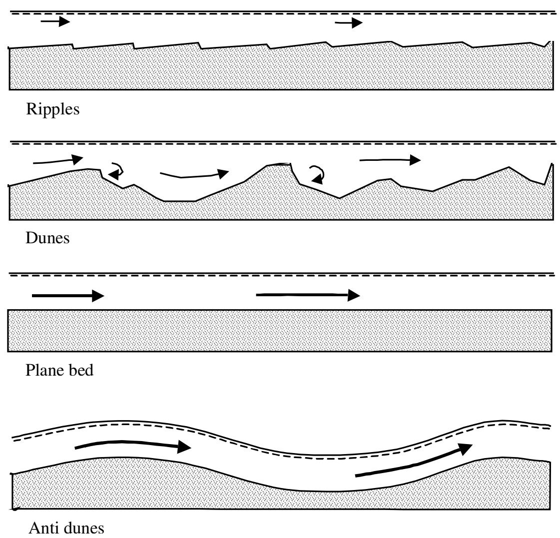

Figure 8 Development of bed forms as the flow velocity increases.

Several hydraulic resistance predictors for alluvial rivers have been proposed, including those of Engelund-Hansen and Ackers & White. Both of these models are semi-empirical linking the hydraulic resistance to the local instantaneous flow conditions. However, there can be a significant lag between the form friction (ie. the bed form size) and the hydraulic conditions. For instance, in many tropical rivers, with distinct dry and wet periods, the sand dunes found at the river bed during the dry season have been formed during a receding flood at the end of the flood season. In such rivers, the hydraulic resistance will often be relatively larger during the dry season. It is therefore important to account for this time lag.

In MIKE 21C, the dynamic development of the bed form size (height and length) has been calculated in some projects with the model developed by Fredsøe (1979). In a subsequent step, the form friction is calculated using a Carnot type formula for expansion loss. The skin friction is determined from a logarithmic boundary layer equation. In quasi-steady flow, this model suggests that as the flow velocity increases, the dune size and hence the hydraulic resistance increases. As the flow velocity increases further, the bed form height and water depth first increase at more or less the same rate and hence the hydraulic resistance only changes slowly until the sand dunes are washed away relatively abruptly and the hydraulic resistance decreases rapidly. These features are illustrated in Figure 8.

For some applications, the differences in bed resistance due to rapidly changing bed levels may be more important than the differences in bed resistance due to increase of decrease in the flow rate. Thus, use of a simpler alluvial bed resistance model was found to be operational in most cases. This model reads (C is the Chezy number, h is the local depth, a and b are calibration constants):

$$C = a \cdot h^b$$

For b=1/6, the model simply equals the Manning formula, whereas for b=0, the model is the Chezy formula. In the morphological model, the depth h will change both as a result of bed level changes and due to water level changes.

Input

The input parameter for the MIKE 21C alluvial resistance model is

- Calibration constants
- Minimum and maximum allowed values of computed bed resistance

Output

The output from the MIKE 21C alluvial resistance model is

- 2D map of bed resistance in a predefined number of timesteps during the simulation time.

BANK EROSION

An important aspect of river morphological processes is bank erosion. For natural rivers without protection of the riverbanks, appropriate description of bank erosion may be vital to get a full picture of the overall morphology of the area. In MIKE 21C, the bank erosion can be simulated in parallel with the sediment transport and hydrodynamic simulations. In each time step, the eroded bank material is included in the solution of the sediment continuity equation. The following bank erosion model is incorporated.

$$E_b = -\alpha \cdot \frac{\partial z}{\partial t} + \beta \cdot \frac{S}{h} + \gamma$$

where

E_b	the bank erosion rate in m/s,
z	local bed level
S	near bank sediment transport
h	local water depth
α,β,γ	calibration coefficients specified in the model

The extra sediment which is discharged into the river from this source and which is included in the sediment continuity equation is (h_b height of the bank above the water level):

$$\Delta S_e = E_b \cdot (h + h_b)$$

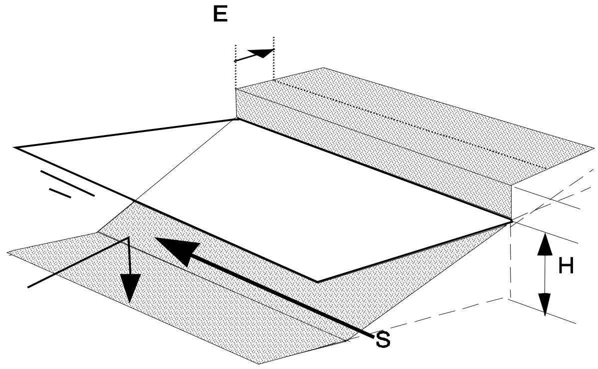

Figure 9 Definition of bank erosion rate E, which in the present model depends on bed level change, sediment transport and depth near the riverbank.

In addition to the formula above, a number of alternative formulations have been tested and is available as hidden features in the MIKE 21C.

The accumulated bank erosion causes a retreat of the bank line position and thereby also in the extent of the modelling area. The MIKE 21C incorporates these plan form changes by re-generating the curvilinear grid during the simulation when the bank line changes exceed a certain pre-defined threshold. In this manner, the morphological model becomes a plan form model.

Input

The input parameter for the MIKE 21C planform model is

- The number and location of eroding banks within the model area (land/water boundary which must follow a curvilinear grid line)
- The erosion characteristics of each eroding bank
- Update frequency of the computational grid due to moving bank lines

Output

The output from the MIKE 21C planform model is

- 2D map of bank erosion in the model area
- 2D map of the co-ordinates of every corner point in each grid cell in the curvilinear mesh at a predefined number of timesteps during the simulation time.

The latter file is similar to the file created with the grid generator, and is applied to depict model results in a movable curvilinear grid.

LARGE SCALE MORPHOLOGY

Large scale in this context means changes in the general bed level within the model boundaries as well as plan form changes due to bank erosion.

The bed and suspended load sediment transport models described earlier in this section predict sediment transport rate and direction. The change of bed level is, therefore, easily determined by integrating the net inflow or outflow within a control volume causing either deposition or scour.

This integration is explicit, due to the non-linear character of the sediment transport relations applied. This implies that the large-scale morphological model needs to be subjected to a rigorous stability criterion for the time step. However, a time step substantially larger than the time step in the hydrodynamic model can generally be applied. In addition, the MIKE 21C has the capability to simulate hydrodynamics assuming quasi-steadiness. With this feature, it is possible to simulate very long time series (years) with even very detailed 2-D models. Finally, the time step for sediment transport simulation can vary automatically by specifying a maximum acceptable sediment transport courant number rather than the time step it self. This option is useful when simulating time series with large variations from low to high flow conditions.

Three kinds of boundary conditions can be specified for the morphological model at the upstream boundary: Total sediment transport, bed level changes, or concentration of suspended sediment (in which case, bed load is calculated explicitly from local hydraulic condition at the boundary). The boundary conditions may vary both in space and time along the boundaries. The effect of bank erosion is included in the sediment continuity equation, ie. the eroded bank material is included as a lateral boundary condition.

The output from the large-scale morphological model is sediment transport (bed load as well as suspended load), the bed level and bed level changes at every grid point and at every time step. Also accumulated bank erosion and new grid co-ordinates are output from the model if the bank erosion and grid update module is activated.

Input

The input parameter for the MIKE 21C Large scale morphology is

- Time series of sediment transport rate, concentration of suspended sediment or bed level changes at the upstream boundary (ASCII file format, Excel or similar). Constants can be defined as well (e.g. bed level changes = 0)
- The number of sediment layers on the river bed
- 2D map (or constant) of the initial sediment layer thickness

- 2D map (or constant) of the initial percentage of each sediment fraction in each layer, if graded sediment is applied.

Output

The output from the MIKE 21C Large scale morphology at a predefined number of timesteps during the simulation time is

- 2D map of bed levels
- 2D map of bed level changes
- 2D map of layer thickness and mean grainsize

Derived results, which can be extracted by a number of graphics based tools are

- Time series and profiles in selected points/lines of bed levels, bed level changes, layer thickness etc.

MODEL VERIFICATION

The MIKE 21C is specially designed for modelling of river morphology. Therefore, it must be able to simulate the development of bend scour, which is one of the main features of meandering rivers as well as development of point bars and alternating bars. In the following, two examples of model applications are presented: One of a flume in a lab, and another of a braided river.

By testing against physical scale modelling results, it is possible to follow the development from a flat, horizontal riverbed. At Delft University of Technology, an extensive number of mobile bed model tests with a curved laboratory flume has been carried out. The results obtained by e.g. Olesen (1987) and Talmon, 1992, have been used for verification of the performance of MIKE 21C.

The u-shaped flume is shown in Figure 9. The width of the flume is 0.50 m. The inflow section (which is straight) has a length of 11 m, the arc length of the bend is 12.9 m, and the radius of curvature of the centre line along the curved section is 4.1 m. The inflow at the upper boundary is constant (5.7 l/s), the average longitudinal slope is 0.0034, the mean depth is 0.048 m, the mean velocity is 0.24 m/s, and the median grain size of the sand in the flume bottom is 0.088 mm.

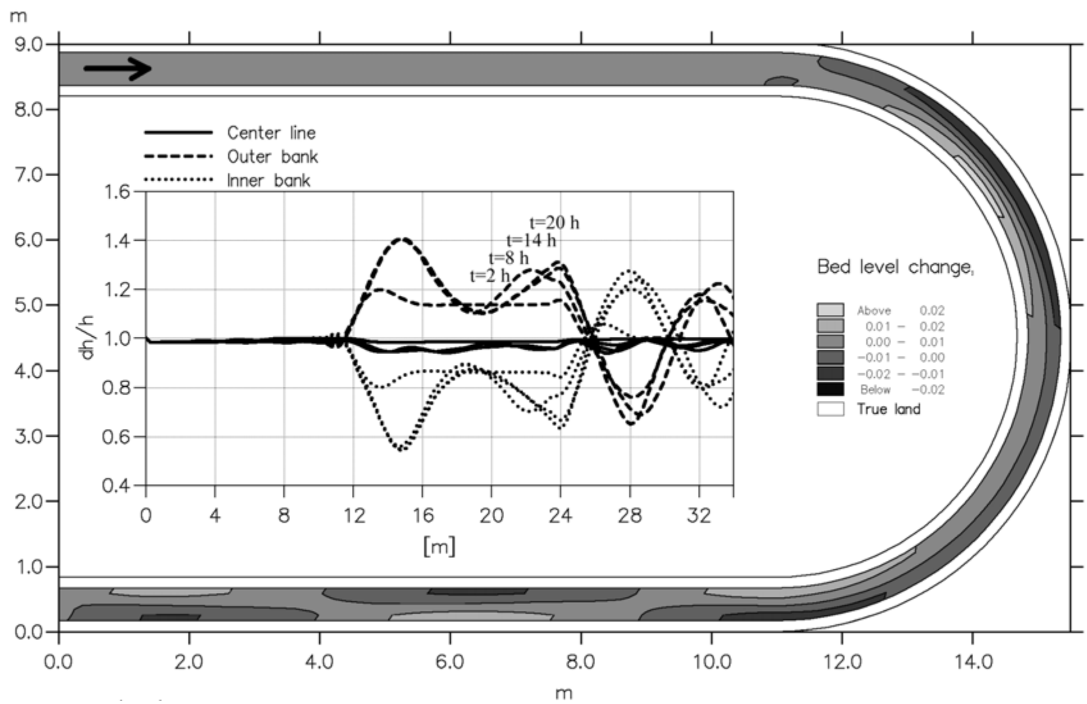

Figure 9 Mathematical model of a laboratory flume. The simulated bed level changes are shown in a plan view together with longitudinal profiles of the time development of the relative depth.

The simulated development of bend scour is clearly seen from Figure 9: Erosion has taken place along the outer bank, and deposition at the inner bank. In the straight reach downstream the curved section, shifting point bars have developed due to the abrupt change in flow (and bank line) curvature. The over-shooting phenomenon in bed levels along river bends is very clearly seen from the results. Finally, the bed level fluctuations (point bars) downstream of the river bend demonstrate the limited numerical damping in the mathematical model and the ability to form a meandering pattern of the channel.

The pattern and magnitude of the bed level change is similar to the observed bed level change from the laboratory flume, see Talmon (1992). As expected, modelling results are sensitive to the chosen parameters for bed slope effect and helical flow effect. From the comparison between the laboratory flume results and the mathematical modelling results, it is evident that the MIKE 21C is capable of reproducing the equilibrium river bend scour as well as the dynamic development bend scour to its mature state.

In the second example, see Figure 10, the model has been used to simulate the development of a braided river. Initially, a completely uniform riverbed with constant slope, discharge, grain size, width, depth, bed resistance has been assumed. Subsequently, the model simulates the development of channels and bars using model parameters similar to those used for calibration of a model of a real river, the Jamuna River in Bangladesh. The simulation covers 30 years.

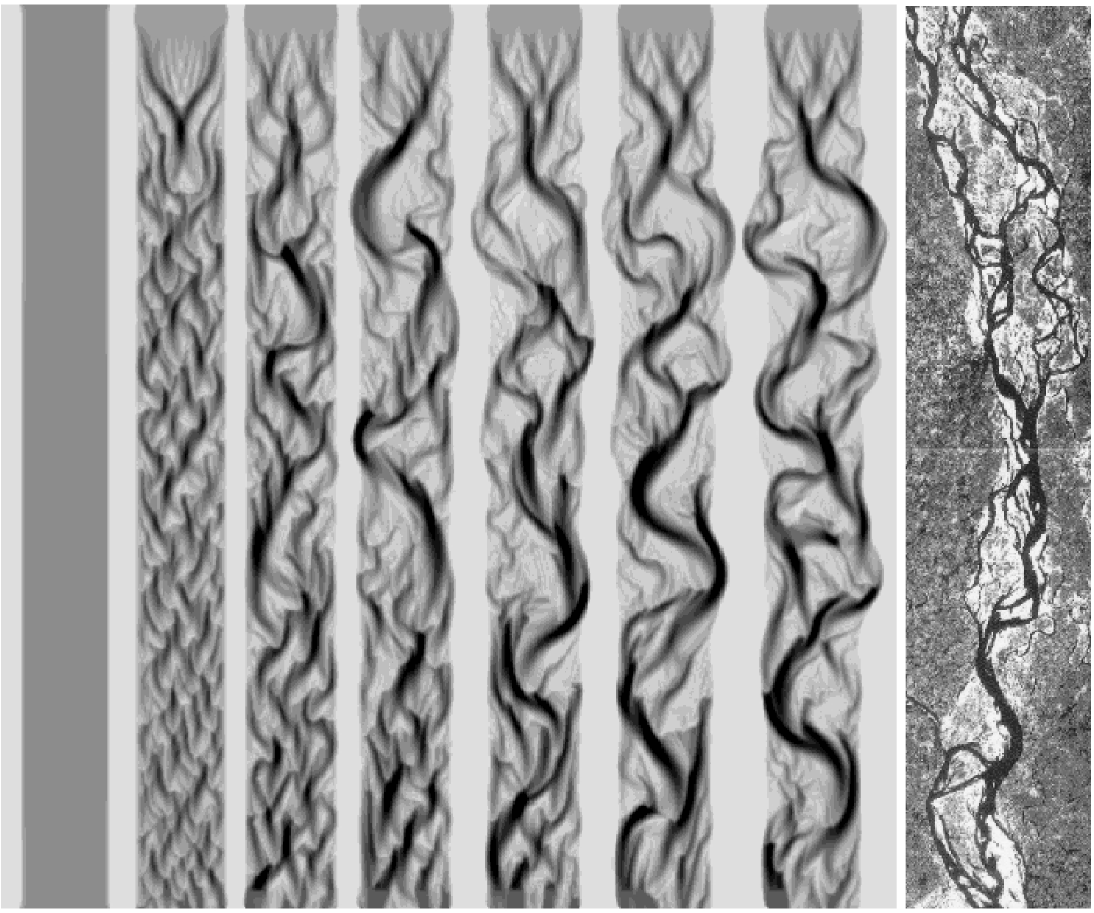

Figure 10 Simulation of a braided river starting with completely uniform conditions (left). The time development is shown after 0, 3, 6, 12, 18, 24, and 30 years. The real braided river (Jamuna River in Bangladesh), from which model parameters were calibrated, is depicted to the left.

Accurate long-term predictions of the morphology of braided rivers cannot be achieved with any model due to the inherent chaotic nature of such rivers. However, in this ultimate test, the MIKE

21C proves to be capable of reproducing the characteristics of the braided river in terms of wave length, braiding intensity, channel width, shape and size of main bars. Only the number of model grid points sets the limit of the resolution of minor channels and bars.

EXAMPLES OF MIKE 21C APPLICATIONS

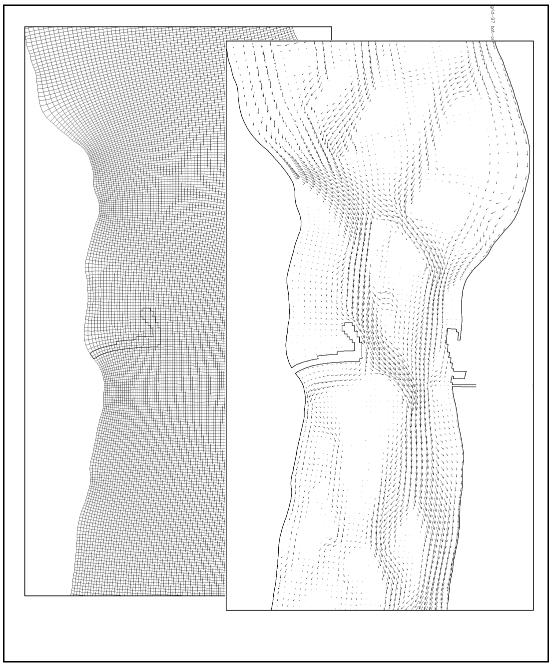

Measurements from the following monsoon were subsequently employed to validate the model simulations (hindcasts) and improve the calibration before the model was applied for another new forecast.

After completion of the bridge, the model is being used to support in Operation and Maintenance of the bridge.

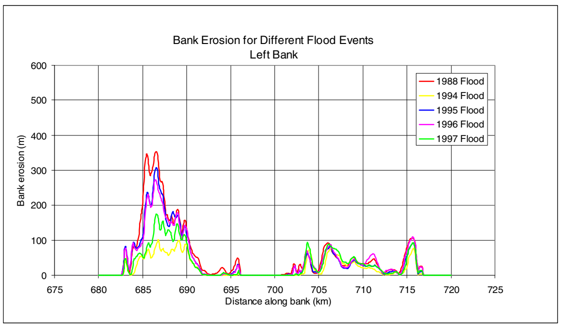

Jamuna River, Bangladesh.

Mathematical modelling was established to provide forecast of critical morphological and hydrodynamic conditions during construction of the Jamuna Multipurpose Bridge 1995-1998.

Measurements of river bathymetry was carried out every year after the monsoon. Subsequently, a model was established of a 36 km reach of the river and applied for predicting flow velocities, water levels, erosion- and deposition rates, bed levels, bank lines etc. in the coming monsoon.

As the actual hydrograph was unknown at the time of simulation, several historical time series of discharge were simulated to cover the possible range of monsoon events.

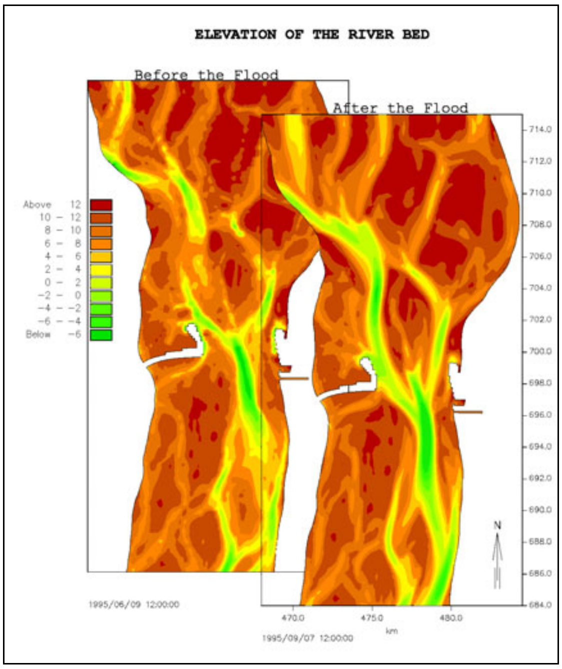

In addition to short-term predictions of critical conditions within the next year, the model of Jamuna was applied to investigate the impact of the bridge project in terms of induced erosion near the river training structures as well as induced increase in water level and flow velocities.

Long-term simulations with MIKE 21C covering 30 years were applied to assess changes in the overall characteristics of the braided Jamuna river due to the bridge.

(Client: World Bank,1995-99)

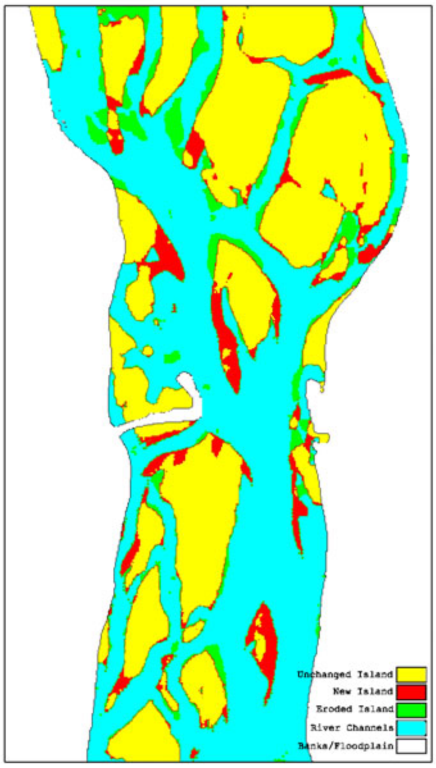

The hydrodynamic model was applied for fish habitat modelling. Simulated results of flow velocities and depths were extracted from the MIKE 21C model to a separate fish habitat model. Sediment transport was modelled as being supply limited because of the presence of a fine sand fraction accumulating in small bars on the armoured gravel riverbed. It was demonstrated how the sediment transport model predicts the impact of reservoirs in terms of effect of a different sediment supply.
(Client: Idaho Power Company, 2000-2002)

Snake River, USA
(right)
The Pine Bar area in the Snake River, Idaho, is considered one of the most important on the river with respect to fish habitat. Also, the sandy bar located on the right riverbank is considered of very high recreational value.

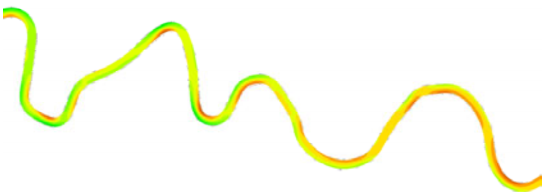

Skjern River, Denmark
(left)
River Skjern was straightened and confined behind embankments through a major regulation in the 60s, which caused a number of negative effects on the environment. In 2001, the restoration of River Skjern was completed- the largest project of its kind in northern Europe. The key objective of the project was to restore the river's original meandering course, to create permanent wetlands, to increase the biodiversity in the river valley, to improve the conditions for trout and salmon and to increase the nutrient turnover in the meadows. MIKE21C was used to assess the morphological equilibrium of the restored river course. (Client: Ministry of Environment, 1998-1999)

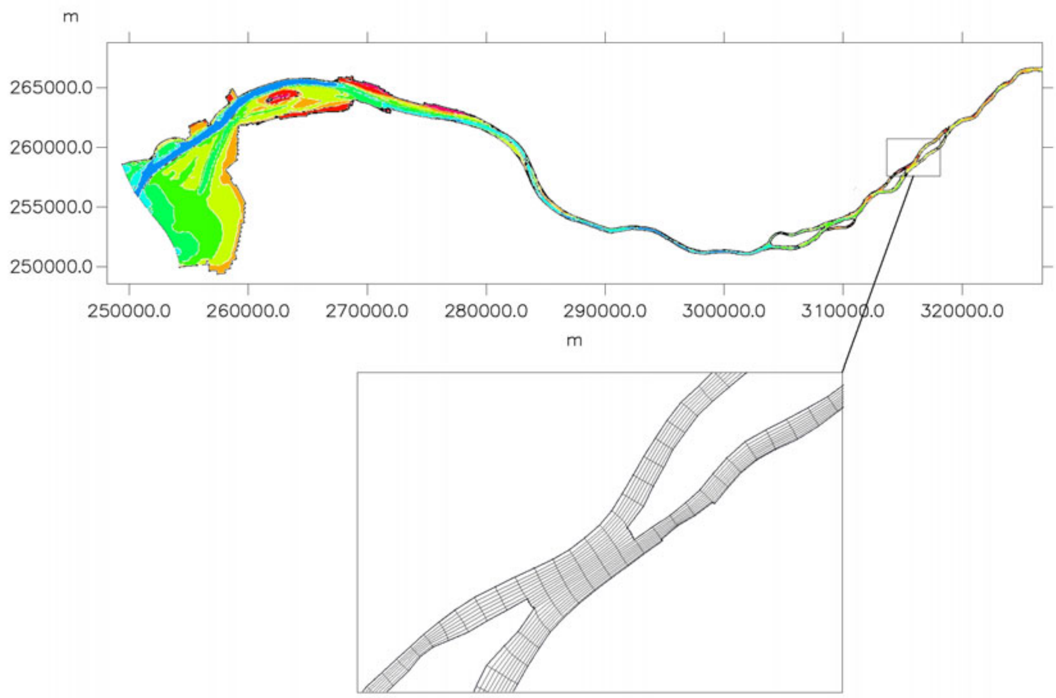

Loire River, France
(above)

In connection with major dredging and river training works in the Loire Estuary, a 2-D model based on MIKE21 CMT was established for predicting changes in hydrodynamics and mud transport. The tidal model was applied for simulating several weeks dynamically in order to evaluate sediment transport patterns over a spring-neap tidal cycle. Boundary conditions were derived from a 1-D MIKE 11 model.

(Client: BCEOM, 1997)

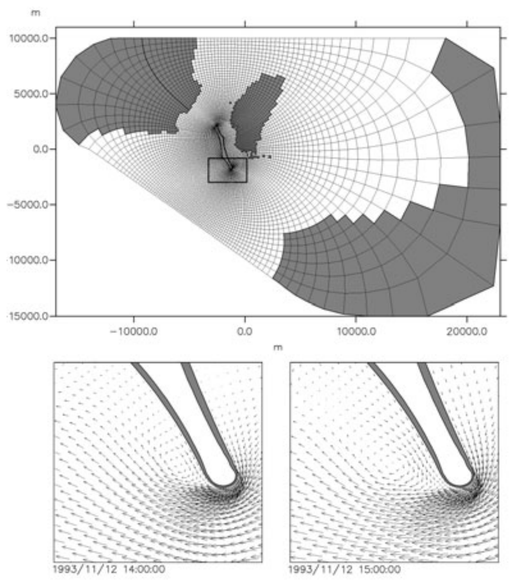

Øresund, Denmark
(left)

A bridge/tunnel link is being constructed across the strait between Sweden and Denmark. Numerous modelling studies have been carried out for design and EIA studies. The present modelling system was applied to investigate the detailed flow pattern around the corners (training walls) of an artificial island in the middle of the strait. The flow is controlled by the water level differences between the Baltic Sea and the North Sea. A curvilinear model was constructed over a larger area (25x20 km) with increasing grid cell intensity towards the training walls under investigation. The minimum grid resolution (5 m) allowed detailed eddy formations to be accurately simulated.

(Client: Øresundskonsortiet, 1998)

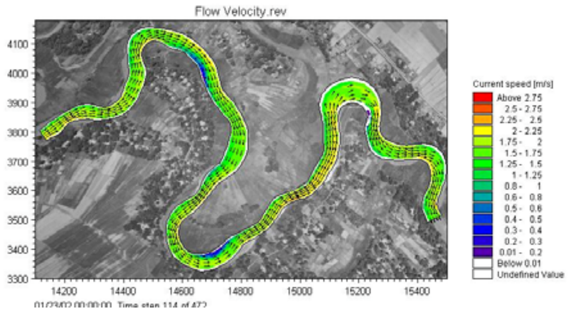

Songwe River, Tanzania/Malawi

(left)
The meandering Songwe River forms part of the physical boundary between the Republic of Malawi and the United Republic of Tanzania and has a length of approximately 200 km. The combination of multi-purpose reservoirs in the upper river basins and bank protection works along the lower reaches has been investigated at a feasibility level. Morphological model tests with MIKE 21C show that management of the frequency and duration of short-term flood events (by means of reservoirs in the middle and upper part of the Songwe River Basin) has a pronounced effect on the overall bank erosion and thereby river stability in downstream reaches.

(Client: Nordic Development Fund, 2001-2003)

Gorai River, Bangladesh

(right)
The supply of fresh water to the South-West region of Bangladesh comes from the Gorai River which is a tributary of the Ganges River. The off-take from the Ganges River has been subject to severe sedimentation in recent years causing the Gorai River to be completely dry in several months each year. With aid from international donors, the Government of Bangladesh has launched a major dredging/river training project to ensure the river stays open.

The MIKE 21C model is applied to 1) assist the main consultant in design of river training works and dredging, 2) assist the dredging company in forecast of short-term morphological conditions, 3) investigate the short-term and long-term impact of river training and dredging.

(Client: Surface Water Modelling Centre, Ministry of Water Resources in Bangladesh, and The World Bank, 1998-99)

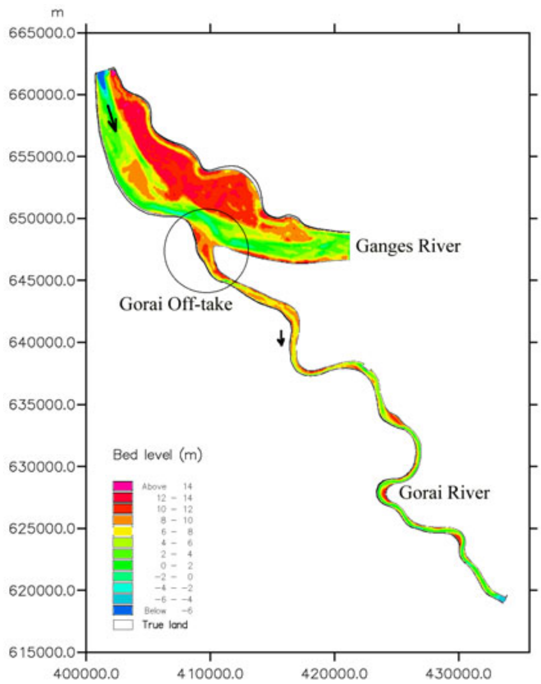

REFERENCES

Ackers, P. and Whit, W.R. (1973) *Sediment Transport: New approach and analysis*, Proc. ASCE, JHD, 99, HY11 pp. 2041-2060

Engelund, F. and Fredsoe, J. (1982) *Hydraulic theory of alluvial rivers*, Advances in Hydro Science, Vol.13, pp.187-215

Engelund, F. and Hansen, E. (1967) *A monograph on sediment transport in alluvial streams*, Teknisk Forlag, Copenhagen

Fredsøe, J. (1979) *Unsteady flow in straight alluvial streams; modifications of individual dunes*, J. Fluid Mech.,Vol. 91, pp 497-512

Galappatti, R. (1983) *A depth integrated model for suspended load*, Communications on Hydraulics 83-7, Dept. Civil Eng. Delft Univ. Tech, The Netherlands

Michelsen, J.A. (1989) *Solution of the Navier-Stokes equations on general non-orthogonal meshes*, FTU/STVF pr J.nr. 95 83 02, Department of Fluid Mechanics, Technical University of Denmark, pp 1-45.

Olesen, K.W. (1987) *Bed topography in shallow river bends*, Faculty of Civil Eng., Delft Univ. Tech., Report 87-1

Ribberink, J.S. (1987) *Mathematical modelling of one-dimensional morphological changes in rivers with non-uniform sediment*"

Rijn, van L.C. (1984a) *Part I: Bed load transport*, J. Hydraulic Eng., 110, 10, October

Rijn, van L.C. (1984a) *Part II: Suspended load transport*, J. Hyd.Eng, 110, 11, November

Talmon, A.M.; Struiksma, N.; van Mierlo, M.C.L.M.; "*Laboratory Measurements of the Direction of Sediment Transport on Transverse Alluvial-bed Slopes*, Journ. of Hydraulic Res., Vol. 33 (1995) no.4

Talmon, A.M. (1992) *Bed topography of river bends with suspended sediment transport*, Faculty of Civil Eng., Delft Univ. Tech., Report 92-5

Vriend, J.J. de (1981) *Steady flow in shallow river bends*, Comm. on Hydraulics 81-3, Dept. Civil Eng.,Delft Univ. Tech., The Netherlands

Wang, Z.B. (1989) *Mathematical Modelling of morphological processes in estuaries*, Report No. 89-1, Faculty of Eng.,Delft Univ. Tech., The Netherlands

Stone (1968) *Iterative Solution of Implicit Approximations of Multidimentional Partial Differential Equations*, SIAM Journal Num. Anal., Vol. 5, No. 3, pp 530-559